Dynamic Responses Comparison of Control Techniques of BDFRG based WECS

Ahmed K. Ibrahim, Mostafa I. Marei, Hamdy S. El-Goharey

Abstract— This paper presents a dynamic analysis study of brushless doubly fed reluctance generator (BDFRG) used for wind energy conversion system (WECS). Scalar (V/F), field-oriented control (FOC), vector control (VC), and direct torque control (DTC) techniques are considered in this study. The system response to various disturbances such as reference speed, load torque, and grid voltage are analyzed for different control techniques using MATLAB/SIMULINK simulation program. Hypothetical step change signals are simulated for the various disturbances to evaluate the dynamic performance of different control techniques used for the BDFRG.

Index Terms— Brushless Doubly Fed Reluctance Generator (BDFRG), WECS, Scalar control, Field Oriented Control (FOC), Direct Torque Control (DTC), Vector Control (VC), Transient Response.

u

1 Introduction

BDFRG represents a promising generator design for wind energy generation systems WEGS specially in offshore applications due to its brushless design which doesn't require transferring of electrical power between movable and fixed parts as both of its primary and secondary windings lies on the same stator core. This unique design gives BDFRG the advantage of doubly fed induction generator DFIG which is the most commonly used generator design for WEGS. In addition, the absence of brushes increases the reliability of the BDFRG which is not the case of DFIG. One more advantage of BDFRG is its ability to operate as an induction generator if it secondary winding is shorted which can be utilized in case of inverter failure "fail-safe mode of operation". On the other hand, the main drawbacks of BDFRG are the large machine size due to its low torque to volume ratio, complex rotor design and complex controllability [1].

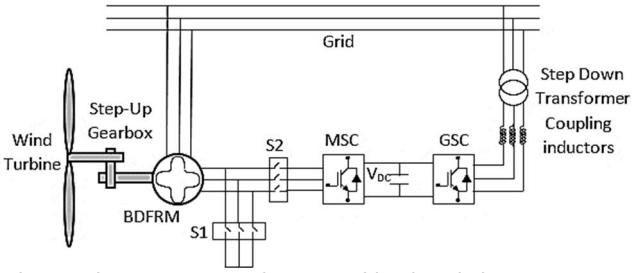

Fig.1. Main Components of BDFRG drive for wind energy conversion system

As mentioned above, the BDFRG contains two standard three-phase windings on the same stator core with different number of poles. One is called the primary or the power winding and is connected directly to the grid, while the other is connected indirectly through a back to back converter. The primary winding handles the main power and the secondary or the control winding handles only slip power. The back to back converter is controlled to achieve desired performance according to control technique utilized. Fig.1 shows detailed construction of BDFRG drive system. The rotor is a salient pole reluctance iron rotor with number of poles equal to summation of pole pairs of both stator windings. In [2 to 13], different control techniques are applied to BDFRG including scalar or V/F, FOC, VC, and DTC which are explained briefly in the next section. This paper is arranged as follow; In section 2, the d-q model using natural frames is explained. Section 3 briefly describes different methods of control for BDFRG. The simulation study is conducted in section 4 while the final conclusion of paper is given in section 5.

2 BDFRG Dynamic Model

As the primary and secondary windings of the BDFRG are fed with two different frequencies, the dynamic equations for these windings are usually referred to two rotating frames ω_p and ω_s; where $\omega_p = 2\pi f_p$ and $\omega_s = 2\pi f_s$ are primary and secondary supply radial frequencies, respectively, where f_p and f_s are primary and secondary frequencies in Hz respectively. Thus, the dynamic model of BDFRG can be describes by:

$$\hat{v}_{p_r} = R_p \hat{\imath}_{p_r} + \frac{d\hat{\lambda}_{p_r}}{dt} + j\omega_p \hat{\lambda}_{p_r} \quad (1)$$

$$\hat{v}_{s_r} = R_s \hat{\imath}_{s_r} + \frac{d\hat{\lambda}_{s_r}}{dt} + j\omega_s \hat{\lambda}_{s_r} \quad (2)$$

$$\hat{\lambda}_{p_r} = L_p \hat{\imath}_{p_r} + L_{ps} \hat{\imath}^*_{s_r} \quad (3)$$

$$\hat{\lambda}_{s_r} = L_s \hat{\imath}_{s_r} + L_{ps} \hat{\imath}^*_{p_r} \quad (4)$$

And the mechanical equation of the machine is:

$$T_e = T_L + J\frac{d\omega_{rm}}{dt} + F\frac{d\omega_{rm}}{dt} \quad (5)$$

where $\hat{v}_{p_r}, \hat{\imath}_{p_r}, \hat{\lambda}_{p_r}$ are the primary winding voltage, current, and flux linkage vectors in the primary rotating frame, respectively, $\hat{v}_{s_r}, \hat{\imath}_{s_r}, \hat{\lambda}_{s_r}$ are the secondary voltage, current, and flux linkage vectors in the secondary rotating frame, respectively, R_p, R_s are the primary and secondary winding resistances, respectively, L_p, L_s, L_{ps} are the primary and secondary windings

· *Ahmed K. Ibrahim is currently pursuing a Ph.D. degree program in electric power and machines department, Ain-Shams University, Cairo, Egypt, PH-+201003168238. E-mail: ahkhibess@yahoo.com*
· *Mostafa I. Marei is a Professor with the Department of Electrical Power and Machines, Ain Shams University, Cairo, Egypt, PH-+201006957052. E-mail: mostafamarei@yahoo.ca*
· *Hamdy S. El-Goharey is a Professor Emeritus with Electrical Power and Machines Department, Ain-Shams University, Cairo, Egypt, PH-+201006066128. E-mail: hamdyk@hotmail.com*

self and mutual inductances, respectively, T_e is the electromagnetic torque of the BDFRG, $T_L$is load torque, and ω_{rm} is the rotor mechanical angular speed.

3 BDFRG CONTROL TECHNIQUES

In this paper, four types of control systems are covered, scalar or V/F, FOC, VC, and DTC. In this section, brief derivation of each control technique is presented.

3.1 BDFRG SCALAR OR V/F CONTROL TECHNIQUE

Scalar control of BDFRG is the simplest and easiest control type. It is suitable only for slow response and narrow speed variations applications. It is mainly driven from steady state equations of BDFRG. Steady state equation can be obtained by setting $\left(\frac{d\hat{\lambda}_{p_r}}{dt} = 0\right)$ and $\left(\frac{d\hat{\lambda}_{s_r}}{dt} = 0\right)$ in equations (1) and (2) respectively. Thus,

$$\hat{v}_{p_r} = R_p\hat{\imath}_{p_r} + j\omega_p\hat{\lambda}_{p_r} \quad (6)$$

$$\hat{v}_{s_r} = R_s\hat{\imath}_{s_r} + j\omega_s\hat{\lambda}_{s_r} \quad (7)$$

As primary winding is supplied from the grid, voltage drop due to primary winding resistance can be ignored if compared to primary winding voltage $\hat{v}_{p_r}$, from (6):

$$\hat{\lambda}_{p_r} = -j\frac{\hat{v}_{p_r}}{\omega_p} \quad (8)$$

Taking the conjugate of (3) and re-arrange;

$$L_{ps}\hat{\imath}^*_{p_r} = \frac{L_{ps}}{L_p}\hat{\lambda}^*_{p_r} - \frac{L^2_{ps}}{L_p}\hat{\imath}_{s_r} \quad (9)$$

From (8) and (9);

$$L_{ps}\hat{\imath}^*_{p_r} = j\frac{L_{ps}}{L_p}\frac{\hat{v}^*_{p_r}}{\omega_p} - \frac{L^2_{ps}}{L_p}\hat{\imath}_{s_r} \quad (10)$$

From (4) and (10);

$$\hat{\lambda}_{s_r} = L_s\hat{\imath}_{s_r} - \frac{L^2_{ps}}{L_p}\hat{\imath}_{s_r} + j\frac{L_{ps}}{L_p}\frac{\hat{v}^*_{p_r}}{\omega_p} \text{ thus,}$$

$$\hat{\lambda}_{s_r} = \sigma L_s\hat{\imath}_{s_r} + j\frac{L_{ps}}{L_p}\frac{\hat{v}^*_{p_r}}{\omega_p} \quad (11)$$

where, $\sigma = 1 - \frac{L^2_{ps}}{L_pL_s}$= secondary winding leakage factor.

Substitute in (7);

$\hat{v}_{s_r} = R_s\hat{\imath}_{s_r} + j\omega_s\left(\sigma L_s\hat{\imath}_{s_r} + j\frac{L_{ps}}{L_p}\frac{\hat{v}^*_{p_r}}{\omega_p}\right)$ or in d-q frame:

$$v_{sd} = R_si_{sd} - \omega_s\sigma L_si_{sq} - \frac{L_{ps}}{L_p}\frac{\omega_s}{\omega_p}v_{pd} \quad (12)$$

$$v_{sq} = R_si_{sq} + \omega_s\sigma L_si_{sd} + \frac{L_{ps}}{L_p}\frac{\omega_s}{\omega_p}v_{pq} \quad (13)$$

Aligning primary rotating frame, thus $v_{sd} = zero$, and ignoring effect of i_{sd} on secondary voltage magnitude as for narrow speed ranges f_s becomes small and thus the term $(\omega_s\sigma L_si_{sd})$ can be ignored so,

$$V_s = R_si_{sq} + \frac{L_{ps}}{L_p}\frac{\omega_s}{\omega_p}v_{pq} = v_{boost} + \frac{V}{F}f_s \quad (14)$$

where $v_{boost} = R_si_{sq}$ which can be set as 10% of rated voltage without a great effect on control performance as stated in [3], and $\frac{V}{F} = \frac{L_{ps}}{f_pL_p}$= constant. According to [16], the BDFRG produces useful torque or power only if:

$$\omega_r = p_r\omega_{rm} = \omega_p + \omega_s \quad (15)$$

The idea of this control is to adjust ω_s according to desired speed command ω^*_{rm}. Therefore, the machine speed is adjusted to fulfill condition of useful torque production (15) and using $\frac{V}{F}$ ratio. The secondary voltage magnitude command v^*_s is calculated and adjusted by controlling the secondary winding inverter.

3.2. BDFRG FIELD-ORIENTED CONTROL FOC TECHNIQUE

The FOC is one of the most important types of control due to decoupled control torque and primary winding (line) reactive power [4], [6], [7] and thus primary power factor control. Writing equations (1) to (4) in d-q forms:

$$v_{pd} = R_pi_{pd} + \frac{d\lambda_{pd}}{dt} - \omega_p\lambda_{pq} \quad (16)$$

$$v_{pq} = R_pi_{pq} + \frac{d\lambda_{pq}}{dt} + \omega_p\lambda_{pd} \quad (17)$$

$$v_{sd} = R_si_{sd} + \frac{d\lambda_{sd}}{dt} - \omega_s\lambda_{sq} \quad (18)$$

$$v_{sq} = R_si_{sq} + \frac{d\lambda_{sq}}{dt} + \omega_s\lambda_{sd} \quad (19)$$

$$\lambda_{pd} = L_pi_{pd} + L_{ps}i_{sd} \quad (20)$$

$$\lambda_{pq} = L_pi_{pq} - L_{ps}i_{sq} \quad (21)$$

$$\lambda_{sd} = L_si_{sd} + L_{ps}i_{pd} \quad (22)$$

$$\lambda_{sq} = L_si_{sq} - L_{ps}i_{pq} \quad (23)$$

where v_{pd}, v_{pq} are primary voltage direct and quadrature components, v_{sd}, v_{sq} are secondary voltage direct and quadrature components, i_{pd}, i_{pq} are primary current direct and quadrature components, i_{sd}, i_{sq} are secondary current direct and quadrature components, λ_{pd}, λ_{pq} are primary flux linkage direct and quadrature components, λ_{sd}, λ_{sq} are secondary flux linkage direct and quadrature components.

Calculating the apparent power for primary and secondary winding:

$$S_p = \frac{3}{2}\hat{v}_{p_r}\hat{\imath}^*_{p_r} = \frac{3}{2}\left(R_pi_p^2 + \hat{\imath}^*_{p_r}\frac{d\hat{\lambda}_{p_r}}{dt} + j\omega_p\hat{\lambda}_{p_r}\hat{\imath}^*_{p_r}\right) \quad (24)$$

$$S_s = \frac{3}{2}\hat{v}_{s_r}\hat{\imath}^*_{s_r} = \frac{3}{2}\left(R_si_s^2 + \hat{\imath}^*_{s_r}\frac{d\hat{\lambda}_{s_r}}{dt} + j\omega_s\hat{\lambda}_{s_r}\hat{\imath}^*_{s_r}\right) \quad (25)$$

At steady state, both $\frac{d\hat{\lambda}_{p_r}}{dt}$ and $\frac{d\hat{\lambda}_{s_r}}{dt}$ vanish. Thus,

$$S_p = \frac{3}{2}\left(R_pi_p^2 + j\omega_p\hat{\lambda}_{p_r}\hat{\imath}^*_{p_r}\right) \quad (26)$$

$$S_s = \frac{3}{2}\left(R_si_s^2 + j\omega_s\hat{\lambda}_{s_r}\hat{\imath}^*_{s_r}\right) \quad (27)$$

The terms $R_pi_p^2$ and $R_si_s^2$ express the copper losses of both primary and secondary windings, respectively. While $j\omega_p\hat{\lambda}_{p_r}\hat{\imath}^*_{p_r}$ and $j\omega_s\hat{\lambda}_{s_r}\hat{\imath}^*_{s_r}$ are the electromechanical active and reactive power components. Thus, rotational active and reactive power components for both primary and secondary winding in d-q forms can be excessed as:

$$P_p = \frac{3}{2}\omega_p(\lambda_{pd}i_{pq} - \lambda_{pq}i_{pd}) \quad (28)$$

$$Q_p = \frac{3}{2}\omega_p(\lambda_{pd}i_{pd} + \lambda_{pq}i_{pq}) \quad (29)$$

$$P_s = \frac{3}{2}\omega_s(\lambda_{sd}i_{sq} - \lambda_{sq}i_{sd}) \quad (30)$$

$$Q_s = \frac{3}{2}\omega_s(\lambda_{sd}i_{sd} + \lambda_{sq}i_{sq}) \quad (31)$$

If primary rotating frame is aligned to primary flux linkage thus, $\lambda_{pq} = zero$. Substituting in (20) and (21);

$\hat{\lambda}_{p_r} = \lambda_p = L_pi_{pd} + L_{ps}i_{sd}$ or,

$$i_{pd} = \frac{1}{L_p}\left(\lambda_p - L_{ps}i_{sd}\right) \quad (29)$$

Also, $L_pi_{pq} - L_{ps}i_{sq} = zero$ or,

$$i_{pq} = \frac{L_{ps}}{L_p}i_{sq} \quad (30)$$

From (4), (22), (23), (29) and (30);

$$\hat{\lambda}_{s_r} = \underbrace{\sigma L_s i_{sd} + \frac{L_{ps}}{L_p}\lambda_p}_{\lambda_{sd}} + j\underbrace{\sigma L_s i_{sq}}_{\lambda_{sq}} \quad (31)$$

$$\text{Or, } \hat{\lambda}_{s_r} = \underbrace{\sigma L_s \hat{i}_{s_r}}_{leakage\ flux} + \underbrace{\frac{L_{ps}}{L_p}\lambda_p}_{mutual\ flux\ \lambda_{ps}} \quad (32)$$

For accurate alignment, knowledge of primary winding resistance is mandatory. Equation (32) shows that by alignment of primary rotating frame to primary flux linkage, the secondary rotating frame is automatically aligned to secondary mutual flux linkage component. Substitute in (28) to (30):

$$P_p = \frac{3}{2}\omega_p \frac{L_{ps}}{L_p}\lambda_p i_{sq} \quad (33)$$

$$Q_p = \frac{3}{2}\frac{\omega_p \lambda_p}{L_p}\left(\lambda_p - L_{ps} i_{sd}\right) \quad (34)$$

$$P_s = \frac{3}{2}\omega_s \frac{L_{ps}}{L_p}\lambda_p i_{sq} = \frac{\omega_p}{\omega_s}P_p \quad (35)$$

Using (15), (33), and (35), the electromagnetic torque can be calculated as follow:

$$T_{em} = \frac{P_o}{\omega_{rm}} = \frac{P_p + P_s}{\omega_{rm}} = \frac{3}{2}p_r \frac{L_{ps}}{L_p}\lambda_p i_{sq} \quad (36)$$

Equation (36) states that the electromagnetic torque can be controlled by controlling i_{sq} only as λ_p is almost constant as primary winding voltage is constant since the primary winding is connected directly to the grid. Thus, the maximum torque per inverter ampere (MTPIA) control strategy can be achieved if i_{sd} is set to zero as it has effect on the torque produced.

Equation (34) states that primary power factor can be controlled by controlling i_{sd} only. Thus, unity primary power factor (UPPF) control strategy can be achieved if ($i_{sd} = \lambda_p / L_{ps}$) so Q_p= zero. From (34) and (36), decoupled control is completely achieved using FOC and this is one of the main advantages of using this type of control. This action is on the expense of complex calculation required for transformations calculations and accurate primary flux angle estimation for frame alignment required.

3.3 BDFRG VECTOR CONTROL VC TECHNIQUE

Vector control shares the same de-coupled control advantage of FOC and doesn't require the knowledge of primary winding resistance. The parameters independent feature of the VC results from aligning the primary voltage vector with the quadrature axis of the primary rotating frame unlike the FOC technique where the primary flux linkage vector is aligned to direct axis. Consequently, the primary flux linkage is slightly shifted from the direct axis due to primary resistance effect as $\lambda_{pd} \gg \lambda_{pq}$. This shift has an ignored effect on controller performance so λ_{pq} can be ignored specially for larger machines where primary resistance is too small and same rules of FOC technique can be applied for VC.

3.4 BDFRG DIRECT TORQUE CONTROL DTC TECHNIQUE

DTC control technique utilizes the same concept of FOC but the alignment of the primary rotating frame to the primary flux linkage is done directly from the stationary frame without the need for any transformation calculations. Returning to equations (31) and (36):

$$T_{em} = \frac{3}{2}\frac{p_r L_{ps}}{L_p}\lambda_{pd} i_{sq} = \frac{3}{2}\frac{p_r L_{ps}}{\sigma L_s L_p}\lambda_p \lambda_{sq} = \frac{3}{2}\frac{p_r}{\sigma L_s}\lambda_{ps}\lambda_s \sin\delta \quad (37)$$

where $\delta = \sin^{-1}\frac{\lambda_{sq}}{\lambda_s}$ is the angular position of the secondary flux linkage in the secondary rotating frame. Equation (37) is the main principle of the DTC. It shows that the torque of the BDFRG can be controlled by controlling secondary flux linkage angle δ in the secondary rotating frame. Alternatively, the secondary flux linkage angle in stationary frame, $\delta + \theta_s$, can be used to control the torque, where $\theta_s = \int \omega_s dt$ is the secondary rotating frame angle. It can be assumed to be constant during the sampling time due to the low frequency of the secondary winding of the BDFRG. As a result, there is no need to determine the position of the secondary winding frame for the DTC as the secondary flux linkage can be directly controlled in the stationary frame. As λ_{ps} or λ_p are constants, depend on primary voltage, the electromagnetic torque can be controlled by controlling the angle δ from stationary frame while keeping λ_s at a desired level to achieve either MTPIA or UPPF strategy.

In this control technique, rotor speed ω_r is measured or estimated and compared with the speed command ω_r^* where the speed error is processed by a simple PI controller to obtain the instantaneous torque command T_{em}^*. This torque command is compared with estimated machine instantaneous torque T_{em} to generate the torque error ΔT_{em}. The estimated instantons torque can be calculated in the stationary frame from [18]:

$$T_{em} = \frac{3}{2}p_r\left(i_{p_\beta}\lambda_{p_\alpha} - i_{p_\alpha}\lambda_{p_\beta}\right) \quad (38)$$

where i_{p_α} and i_{p_β} are primary current components in stationary $\alpha\beta$ frame, λ_{p_α} and λ_{p_β} are primary flux linkage components in stationary $\alpha\beta$ frame, and are calculated as follow:

$$\lambda_{p\alpha} = \int\left(v_{p\alpha} - R_p i_{p\alpha}\right)dt \quad (39)$$

$$\lambda_{p\beta} = \int\left(v_{p\beta} - R_p i_{p\beta}\right)dt \quad (40)$$

$$\lambda_p = \sqrt{\lambda_{p\alpha}^2 + \lambda_{p\beta}^2} \quad (41)$$

where v_{p_α} and v_{p_β} are secondary voltage components in stationary frame, i_{p_α} and i_{p_β} are secondary current components in stationary frame, λ_{p_α} and λ_{p_β} are secondary flux linkage components in stationary frame. The command of the secondary flux linkage λ_s^* is set at its optimum value which is based on the required control strategy, UPPF or MTPIA. It had been shown that for UPPF, the desired secondary flux linkage can be expressed as [13, 14]:

$$\lambda_s^* = \sqrt{\left(\frac{L_s}{L_{ps}}\lambda_p\right)^2 + \left(\frac{\sigma L_{ps}}{1-\sigma} \times \frac{2T_{em}^*}{3p_r\lambda_p}\right)^2} \quad (42)$$

In contrast, the desired secondary flux linkage to achieve MTPIA can be expressed as [10, 12]:

$$\lambda_s^* = \sqrt{\lambda_{ps}^2 + \left(\frac{\sigma L_{ps}}{1-\sigma}\frac{2T_{em}^*}{3p_r\lambda_p}\right)^2} \quad (43)$$

Depending on selected control strategy, the desired secondary flux linkage λ_s^* is compared with the estimated instantaneous secondary flux linkage λ_s and the error $\Delta\lambda_s$ is generated. The estimated secondary instantaneous flux linkage λ_s and flux angle in stationary frame are estimated as follow:

$$\lambda_{s\alpha} = \int (v_{s\alpha} - R_s i_{s\alpha})\, dt \quad (44)$$

$$\lambda_{s\beta} = \int (v_{s\beta} - R_s i_{s\beta})\, dt \quad (45)$$

$$\lambda_s = \sqrt{\lambda_{s\alpha}^2 + \lambda_{s\beta}^2} \quad (46)$$

$$\delta + \theta_s = \tan^{-1} \frac{\lambda_{s\beta}}{\lambda_{s\alpha}} \quad (47)$$

where v_{s_α} and v_{s_β} are secondary voltage components in stationary frame, i_{s_α} and i_{s_β} are secondary current components in stationary frame, λ_{s_α} and λ_{s_β} are secondary flux linkage components in stationary frame. The sector number is then determined according to below:

$$Sector = \begin{cases} 330^o \le (\theta_s + \delta) < 30^0, & Sector\ 1 \\ 30^o \le (\theta_s + \delta) < 90^0, & Sector\ 1 \\ 30^o \le (\theta_s + \delta) < 90^0, & Sector\ 1 \\ 150^o \le (\theta_s + \delta) < 210^0,, & Sector\ 1 \\ 210^o \le (\theta_s + \delta) < 270^0, & Sector\ 1 \\ 270^o \le (\theta_s + \delta) < 330^0, & Sector\ 1 \end{cases} \quad (45)$$

Using sector number, torque error ΔT_{em} and flux linkage error $\Delta\lambda_s$, the switching states for the machine side inverter is determined from switching table 1 [10 to 15].

TABLE 1
DTC SWITCHING TABLE

Comp.		*Sector* 1			*Sector* 2			*Sector* 3			*Sector* 4			*Sector* 5			*Sector* 6		
$\Delta\lambda_s$	ΔT_{em}	a	b	c	a	b	c	a	b	c	a	b	c	a	b	c	a	b	c
0	0	0	0	1	1	0	1	1	0	0	1	1	0	0	1	0	0	1	1
0	1	0	1	0	0	1	1	0	0	1	1	0	1	1	0	0	1	1	0
1	0	1	0	1	1	0	0	1	1	0	0	1	0	0	1	1	0	0	1
1	1	1	1	0	0	1	0	0	1	1	0	0	1	1	0	1	1	0	0

4 SIMULATION RESULTS AND DISCUSSIONS

Simulation study using MATLAB/SIMULINK is performed for the BDFRG with the given parameters in the Appendix. Disturbances in speed, torque, and grid voltage are simulated to evaluate the dynamic response of the four control techniques.

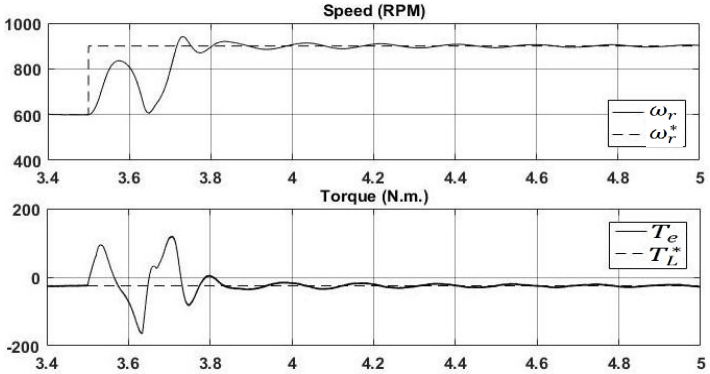

Fig.2 Dynamic response of scalar controlled BDFRG under step change in rotor speed command ω_r^*.

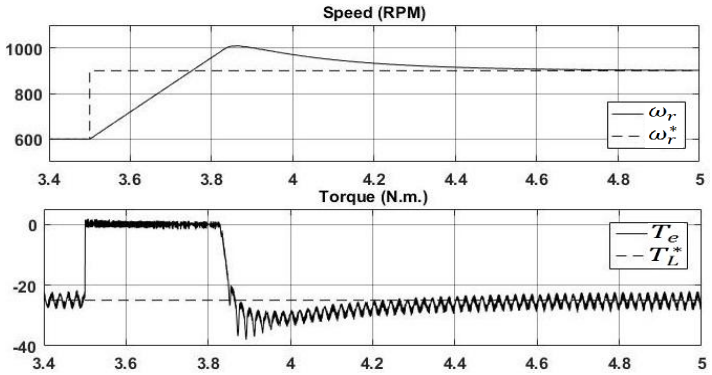

Fig.3 Dynamic response of FOC based BDFRG under step change in rotor speed command ω_r^*.

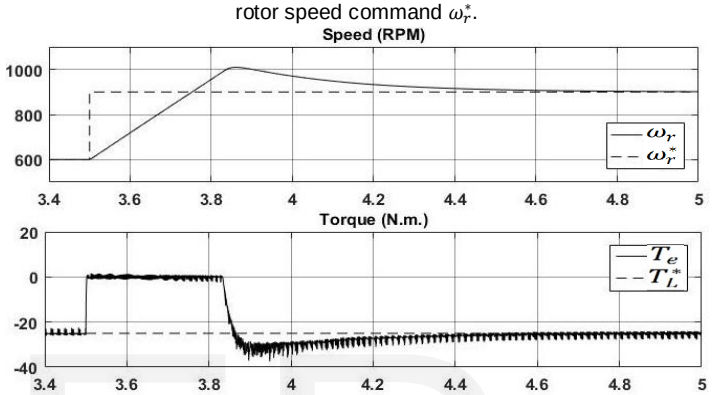

Fig.4 Dynamic response of VC based BDFRG under step change in rotor speed command ω_r^*.

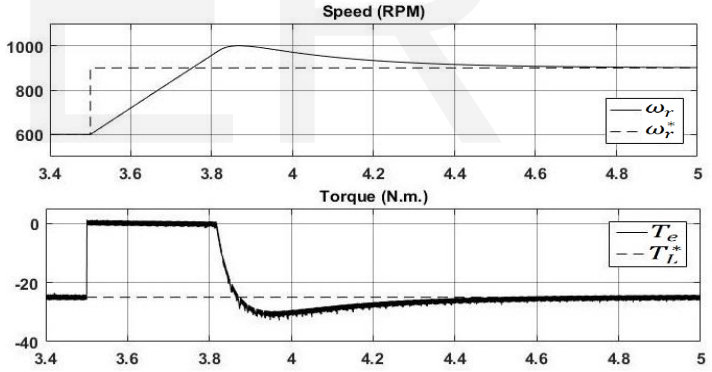

Fig.5 Dynamic response of DTC based BDFRG under step change in rotor speed command ω_r^*.

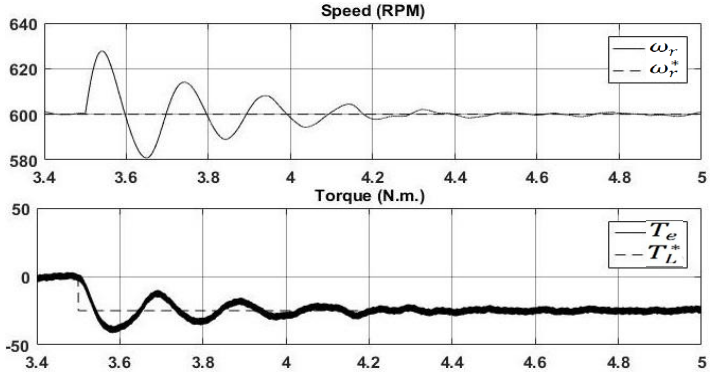

Fig.6 Dynamic response of scalar controlled BDFRG under step change in load torque T_L^*.

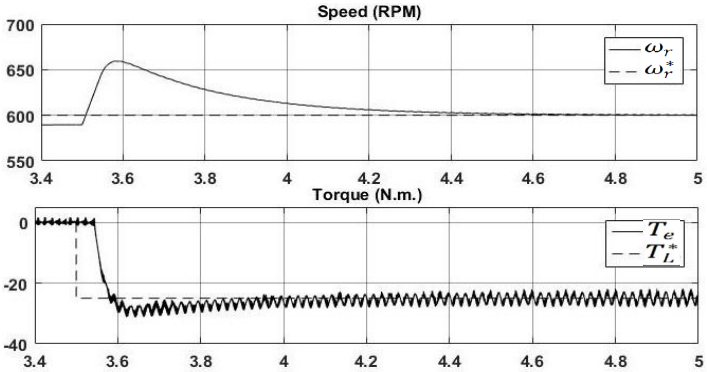

Fig.7 Dynamic response of FOC based BDFRG under step change in load torque T_L^*.

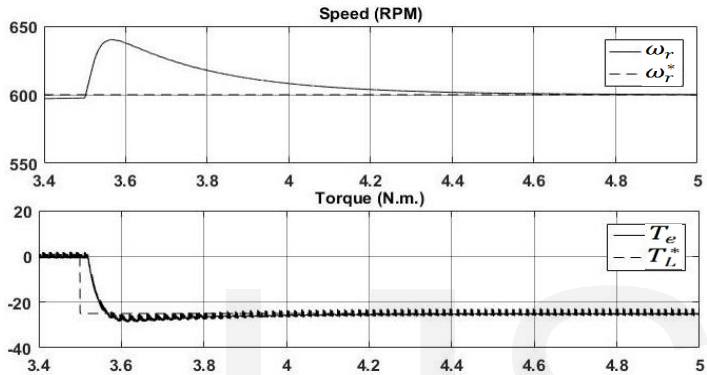

Fig.8 Dynamic response of VC based BDFRG under step change in load torque T_L^*.

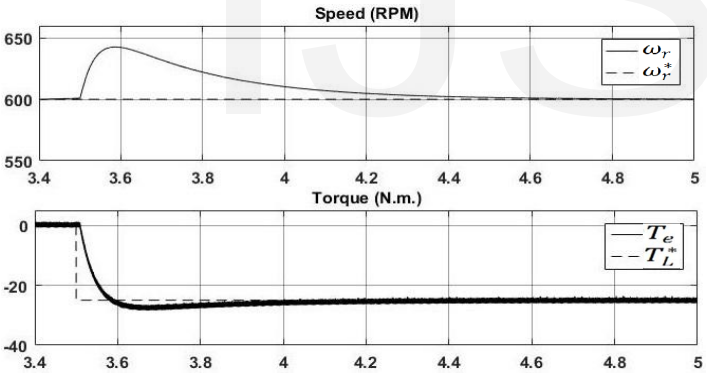

Fig.9 Dynamic response of DTC based BDFRG under step change in load torque T_L^*.

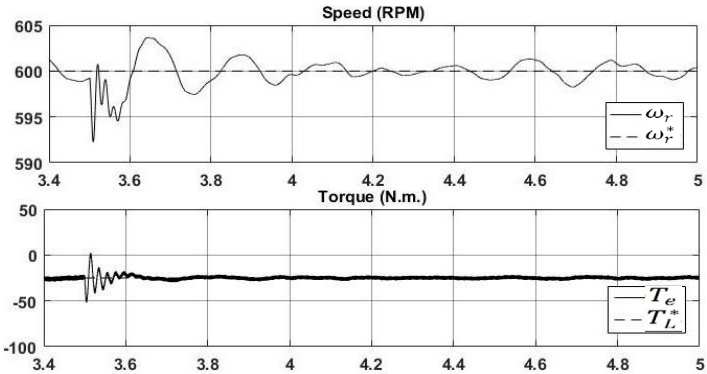

Fig.10 Dynamic response of scalar controlled BDFRG under 20% grid voltage dip.

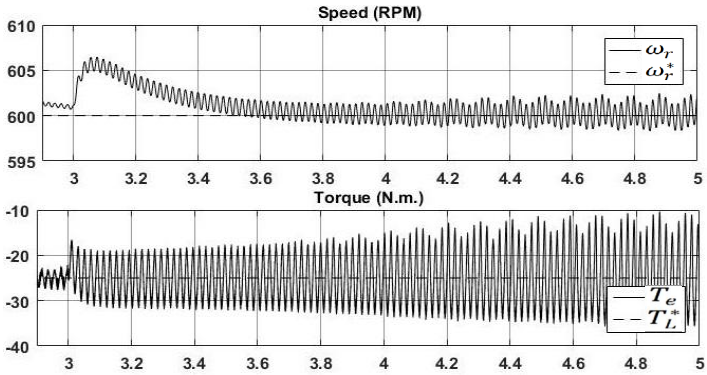

Fig.11 Dynamic response of FOC based BDFRG under 20% grid voltage dip.

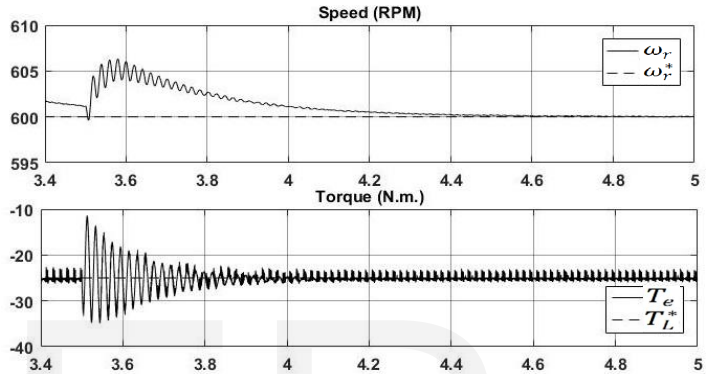

Fig.12 Dynamic response of VC based BDFRG under 20% grid voltage dip.

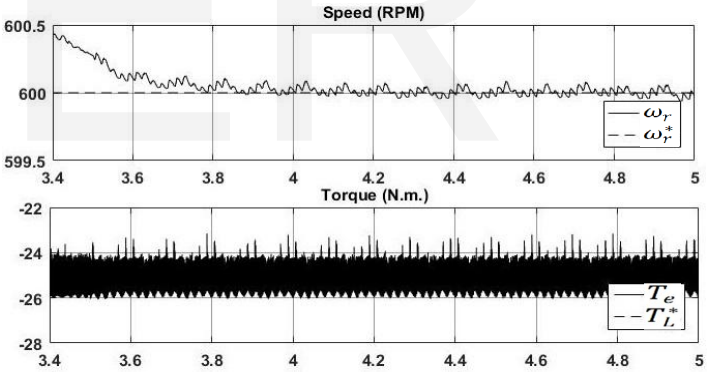

Fig.13 Dynamic response of DTC based BDFRG under 20% grid voltage dip.

Figs. 2, 3, 4, and 5 illustrate the dynamic response of the BDFRG under a step change in speed command from 600 rpm, at sub-synchronous mode, to 900 rpm, at super-synchronous mode. The generator load torque is set at -25 Nm. for different control techniques. The scalar controlled BDFRG showed an underdamped speed and torque response with speed and torque overshoots of 50 rpm and 125Nm. It is noted that the torque jumps to positive 100 Nm during the transition from sub-synchronous mode to super-synchronous mode which is forbidden for WECS. Unfortunately, this action can't be controlled as decoupled control can't be achieved using scalar control. This action makes scalar control not favorable for WECS applications. The FOC, VC, and DTC reveal a nearly identical overdamped transient response for speed with 100 rpm overshoot with smoothest torque response for DTC than

both VC and FOC. It worth to mention that torque controller is limited to zero for FOC, VC, and DTC to prevent positive torque production during transition from sub-synchronous to super-synchronous modes.

Fig. 6, 7, 8, and 9 demonstrate the dynamic response of BDFRG under sudden loading of 25 Nm. from no-load condition at 600 rpm using the four control techniques. Again, underdamped or oscillatory speed and torque responses are observed for scalar control with overshoots in speed and torque of 30 rpm and 12.5 Nm, respectively. FOC shows speed and torque overshoot of 55 rpm and 5 Nm respectively with superimposed torque oscillations of 2 Nm. VC and DTC techniques show nearly identical overdamped speed and torque responses with speed and torque overshooting of 40 rpm and 5 Nm, respectively. The superimposed torque oscillations for VC is less than FOC case, while no or neglectable torque oscillations are observed for DRC.

Finally, Figs. 10, 11, 12, and 13 show the dynamic responses of the BDFRG using the four control techniques under a grid voltage dip of 20%. All control techniques exhibit underdamped torque and speed responses except DTC which is not affected by the grid voltage disturbance. The speed overshoots observed when using scalar control, FOC, VC, and DTC are 7 rpm, 7 rpm, 5 rpm, and 0.5 rpm, respectively. The torque overshooting are 25 Nm, 10 Nm, 12 Nm, and 1 Nm when scalar control, FOC, VC, and DTC are used, respectively.

5 Conclusion

In this paper, the main control techniques used for BDFRG have been briefly explained and simulated successfully. To evaluate their dynamic response, different types of disturbances are considered such as step change in speed command, step change in load torque command, and grid voltage dip. The FOC, VC, and DTC methods show stable responses and acceptable overshooting while scalar control responses weren't acceptable in some cases where positive electromagnetic torque is generated (motoring mode) which is forbidden for WECS applications. FOC and VC methods showed oscillatory responses under voltage dips while DTC method was able to handle voltage dips with neglectable effects on speed and torque responses. It is worth mentioning that DTC method is able to present decoupled control without the need for rotating transformation calculations which is not the case for FOC and VC techniques.

Appendix

The BDFRG machine under study is a 4 kW, 750 rpm, 6/2-pole, Y-connected. The machine primary winding ratings are 415 V, 50 Hz, 7.5 A. The detailed parameters of the machine are listed in Table 2.

TABLE 2

BDFRG Prototype Parameters and Ratings

Symbol	Quantity	Value
J	Rotor inertia	0.2 $kg \cdot m2$
F	Friction coefficient	0
R_p	Primary resistance	3.78 Ω
R_s	Secondary resistance	2.44 Ω
L_{mp}	Primary winding self-inductance	0.41 H
L_{ms}	Secondary self-inductance	0.32 H
L_{psmax}	Mutual inductance	0.3 H
p_r	Rotor poles	4

References

[1] Hyong Sik Kim, Dylan Dah-Chuan Lu, "Wind Energy Conversion System from Electrical Perspective —A Survey", Smart Grid and Renewable Energy, 2010, 1, 119-131.

[2] Mohamed G. Mousa, S. M. Allam, and Essam M. Rashad, "A Sensorless Scalar-Control Strategy for Maximum Power Tracking of a Grid-Connected Wind-Driven Brushless Doubly-Fed Reluctance Generator", 978-1-4673-9130-6/15/$31.00 ©2015 IEEE.

[3] Mohamed Saad Hassan, "Control of Brushless Doubly-Fed Reluctance Machines under Normal and Faulty Operating Conditions", A thesis submitted in partial fulfilment of the requirements of the University of Northumbria at Newcastle for the degree of Doctor of Philosophy, 2014.

[4] MILUTIN JOVANOVI´C and KRISHNA BUSAWON, "Control Methods for Doubly-Fed Reluctance Machines", Proc. of the 5th WSEAS/IASME Int. Conf. on Electric Power Systems, High Voltages, Electric Machines, Tenerife, Spain, December 16-18, 2005 (pp143-148).

[5] Milutin G. Jovanovic, Jian Yu, "Maximum Efficiency Control of Brushless Doubly Fed Reluctance Motors for Large Pump Applications", F. Parasiliti et al. (eds.), Energy Efficiency in Motor Driven Systems © Springer-Verlag Berlin Heidelberg 2003.

[6] Sul Ademi, Milutin G. Jovanovic, Mohammed Hasan, "Control of Brushless Doubly-Fed Reluctance Generators for Wind Energy Conversion Systems", Manuscript received May 13, 2014; revised August 8, 2014; accepted September 15, 2014. Paper no. TEC-00322-2014.

[7] Sul Ademi, Milutin Jovanovic´ and Jude K. Obichere, "Comparative Analysis of Control Strategies for Large Doubly-Fed Reluctance Wind Generators", Proceedings of the World Congress on Engineering and Computer Science 2014 Vol I WCECS 2014, 22-24 October, 2014, San Francisco, USA.

[8] Milutin G. Jovanovic, "A Comparative Study of Control Strategies for Performance

[9] Milutin Jovanovic and Hamza Chaal, "High-Performance Control of Doubly-Fed Reluctance Machines", ELECTRONICS, VOL. 14, 72 NO. 1, JUNE 2010.

[10] M. G. JovanoviC', J. Yu' and E. Levi2, "A Doubly-Fed Reluctance Motor Drive with Sensorless Direct Torque Control", ~7803-7817-2/03/$17.M)B ZW3 IEEE.

[11] Hamza Chaal and Milutin Jovanovic, "A New Sensorless Torque and Reactive Power Controller for Doubly-Fed Machines", XIX International Conference on Electrical Machines - ICEM 2010, Rome.

[12] Milutin G. Jovanovi´c, Senior Member, IEEE, Jian Yu, and Emil Levi, Senior Member, IEEE, "Encoderless Direct Torque Controller for Limited Speed Range Applications of Brushless Doubly Fed Reluctance Motors", IEEE TRANSACTIONS ON INDUSTRY APPLICATIONS, VOL. 42, NO. 3, MAY/JUNE 2006.

[13] Milutin G Jovanovic, David G Dorrell, "Sensorless Control of Brushless Doubly-Fed Reluctance Machines using an Angular Velocity Observer", 1-4244-0645-5/07/$20.00©2007 IEEE.

[14] M. G. Jovanovic and M. M. R. Ahmed, "Sensorless Speed Control Strategy for Brushless Doubly-Fed Reluctance Machines", 1 -4244-0743-5/07/$20.OO ©2007 IEEE

[15] William K Song, "Improved Direct Torque Control of a Brushless Doubly-Fed Reluctance Machine", A thesis submitted in fulfilment of the requirements for the degree of Doctor of Philosophy in the Centre for Electrical Machines and

Power Electronics School of Elec. Mech. & Mechatronics System Faculty of Engineering and IT May 2017, University of Technology, Sydney.

[16] Robert E. Betz and Milutin Jovanvic, "Introduction to Brushless Doubly Fed Reluctance Machines – The Basic Equations", School of Electrical Engineering and Computer Science, University of Newcastle, NSW,2308, Australia, Technical Report: EE0023, March 27,2012.

[17] Ahmed K. Ibrahim, Mostafa I. Marei, Hamdy S. El-Goharey, "Transient Model of Brushless Doubly Fed Reluctance Machine using ABC Reference Frame," International Journal of Recent Trends in Engineering & Research (IJRTER), Volume 04, Issue 11; November - 2018 [ISSN: 2455-1457].